Journal of Modern Optics
Vol. 56, Nos. 2–3, 20 January–10 February 2009, 196–200

Taylor & Francis
Taylor & Francis Group

Constrained MaxLik reconstruction of multimode photon distributions

G. Brida[a]*, M. Genovese[a], A. Meda[a], S. Olivares[b,c], M.G.A. Paris[b,c,d] and F. Piacentini[a]

[a]*Istituto Nazionale di Ricerca Metrologica, Torino, Italy;* [b]*CANIS UdR Milano Università, Milano, Italy;* [c]*Dipartimento di Fisica, Università di Milano, Milano, Italy;* [d]*ISI Foundation, Torino, Italy*

(*Received 13 February 2008; final version received 30 July 2008*)

We address the reconstruction of the full photon distribution of multimode fields generated by seeded parametric down-conversion. Our scheme is based on on/off avalanche photodetection assisted by maximum-likelihood (MaxLik) estimation and does not involve photon counting. We present a novel constrained MaxLik method that incorporates the request of finite energy to improve the rate of convergence and, in turn, the overall accuracy of the reconstruction.

Keywords: reconstruction; photon; statistics; distribution; quantum; PDC

1. Introduction

The reconstruction of photon statistics of quantum optical fields is of the utmost relevance for several applications, ranging from quantum information [1] to the foundations of quantum mechanics [2] and quantum optics [3–7]. Despite this fact, the realization of photodetectors well suited for this purpose still represents an experimental challenge. The few existing examples [8–13] show severe limitations. On the other hand, reconstruction schemes based on quantum tomography [14–16] require phase-matching with a suitable local oscillator and do not represent a technique suited for a diffuse use. This situation has prompted various theoretical studies [17–20] addressed to achieve the reconstruction of the (diagonal) elements of the density matrix exploiting the information achievable with realistic detectors.

In a recent series of papers [21–25], we have demonstrated how a very satisfactory reconstruction of the statistics of mono-partite and bi-partite quantum optical states may be obtained using the simplest kind of detectors, namely on/off detectors [19,20] operating in the Geiger mode, whose outcomes are either 'off' (no photons detected) or 'on', i.e. a 'click' indicating the detection of one or more photons. Our method recovers the full photon statistics using maximum-likelihood (MaxLik) reconstruction on on/off data obtained using variable detection efficiency (by inserting calibrated neutral filters).

In this paper we present a modified version of our method, which improves both convergence and accuracy upon incorporating the obvious *a priori* constraint of finite signal energy. In particular, we address the reconstruction of the full photon distribution of multimode fields generated by seeded parametric down-conversion (PDC). The novel method allows us to overcome the increased complexity of the reconstruction problem and represents an important step in view of the widespread application of MaxLik reconstruction.

The paper is structured as follows. In the next section we explain the constrained MaxLik algorithm in some details, whereas in Section 3 we describe the experimental apparatus and illustrate the application of the method to the reconstruction of the photon distribution of multimode fields generated by seeded PDC. Finally, Section 4 closes the paper with some concluding remarks.

2. Constrained MaxLik algorithm

The probability $p_0(\eta)$ that a photodetector with quantum efficiency η does not click when an input quantum state $\varrho = \sum_{n,m} \varrho_{nm} |n\rangle\langle m|$ impinges on it reads as follows:

$$p_0(\eta) = \sum_n (1-\eta)^n \varrho_n, \tag{1}$$

where $\varrho_n = \varrho_{nn}$ is the nth entry of the photon distribution of the input state. Now, if we consider a set of N detectors with different quantum efficiencies η_ν, $\nu = 1, \ldots, N$, then we can write the 'off' probabilities as

$$\mathtt{P}_\nu \equiv p_0(\eta_\nu) = \sum_n A_{\nu n} \varrho_n, \tag{2}$$

*Corresponding author. Email: g.brida@inrim.it

ISSN 0950–0340 print/ISSN 1362–3044 online

DOI: 10.1080/09500340802389805
http://www.informaworld.com

where $A_{\nu n}=(1-\eta_\nu)^n$. Looking at Equation (2) as a statistical model for the parameters ϱ_n, we can solve it by MaxLik estimation. We proceed as follows: first of all, we assume there exists a value $\tilde{n}$ such that ϱ_n is negligible for $n>\tilde{n}$; then we assign the *loglikelihood* function (with mutually normalized $\mathtt{P}_\nu$), that is the global probability of the sample:

$$\mathtt{L}=\frac{1}{N_x}\log\prod_\nu\left(\frac{\mathtt{P}_\nu}{\sum_\lambda \mathtt{P}_\lambda}\right)^{\mathcal{N}_\nu}=\sum_\nu f_\nu\log\frac{\mathtt{P}_\nu}{\sum_\lambda \mathtt{P}_\lambda}, \tag{3}$$

where $f_\nu=\mathcal{N}_\nu/N_x$ is the experimental frequency of 'off' events, $\mathcal{N}_\nu$ being the number of 'off' events for a fixed quantum efficiency η_ν and N_x the total number of events. The MaxLik estimated ϱ_n values are the ones maximizing $\mathtt{L}$. Since the model is linear and the unknowns ϱ_n are positive, we can find the expectation-maximization solution of the MaxLik problem by means of an iterative procedure as described in [17,21, 26–28], i.e.

$$\varrho_n^{(h+1)}=\frac{\varrho_n^{(h)}}{\sum_m \varrho_m^{(h)}}\sum_\nu\frac{A_{\nu n}}{(\sum_\lambda A_{\lambda n})}\frac{f_\nu}{\mathtt{P}_\nu^{(h)}}, \tag{4}$$

where $\varrho_n^{(h)}$ is the value of ϱ_n evaluated at the hth iteration, and $\mathtt{P}_\nu^{(h)}=\sum_n A_{\nu n}\varrho_n^{(h)}$. The algorithm (4), known to converge unbiasedly to the MaxLik solution, provides a solution once the initial distribution $\varrho_n^{(0)}$ is chosen. On the other hand, the initial distribution slightly affects only the convergence rate and *not* the precision at convergence [19].

As a matter of fact, the solution obtained above corresponds to the best photon distribution fitting the experimental data, i.e. the measured 'off' probabilities. However, it is possible that different photon distributions fit the same experimental data, giving rise to a *family* of *suitable* distributions. In these cases it could happen that the MaxLik solution, even if in good agreement with the available experimental knowledge, may be different from the actual (unknown) one. Indeed, this is the case of multimode fields when the number of modes grows. In order to overcome this limitation, we have developed a modified version of the MaxLik algorithm, which incorporates the constraint of finite energy for the incoming signal, i.e. the quantity $\sum_n n\varrho_n$. In practice, we maximize the loglikelihood (3) with a constraint on the energy. Now the function to be maximized with respect to ϱ_n is

$$\mathtt{L}_\beta=\mathtt{L}-\beta\sum_n n\varrho_n, \tag{5}$$

with $\mathtt{L}$ being given in (3) and β being a Lagrange multiplier. The equations $\frac{\partial \mathtt{L}_\beta}{\partial\varrho_n}=0$ lead to

$$\left(\frac{\sum_\gamma \mathtt{P}_\gamma}{\sum_\mu f_\mu}\right)\sum_\nu\frac{A_{\nu n}}{\left[\sum_\lambda A_{\lambda n}+\beta n\left(\frac{\sum_{\gamma'}\mathtt{P}_{\gamma'}}{\sum_{\mu'}f_{\mu'}}\right)\right]}\frac{f_\nu}{\mathtt{P}_\nu}=1, \tag{6}$$

and, then, by multiplying both sides of Equation (6) by ϱ_n, we get a map $\boldsymbol{T}\,\varrho_n=\varrho_n$, whose fixed point can be obtained by the following iterative solution:

$$\varrho_n^{(h+1)}=\frac{\varrho_n^{(h)}}{\sum_m \varrho_m^{(h)}}\sum_\nu\frac{A_{\nu n}}{\left[\sum_\lambda A_{\lambda n}+\beta n\left(\frac{\sum_{\gamma'}\mathtt{P}_{\gamma'}^{(h)}}{\sum_{\mu'}f_{\mu'}}\right)\right]}\frac{f_\nu}{\mathtt{P}_\nu^{(h)}}. \tag{7}$$

The parameter β can be tuned in order to control the energy of the reconstructed state and improve both the convergence rate and the overall accuracy. Of course, if we take $\beta=0$, then Equations (7) and (4) become the same.

Indeed, in order to use Equation (7) we need to know the input state energy which, in general, cannot be directly accessible from experimental data. However, in cases when a model of the photon distribution of the input state is available, we can estimate *indirectly* this energy by a simple fit of the 'off' probabilities.

Since the mean of the reconstructed statistics can be assessed only at convergence, it is impossible to choose a prior value of β. Our algorithm overcomes this problem in two steps: at first the unconstrained solution ($\beta=0$) and the corresponding energy are evaluated; then, if necessary, the value of β is incrementally tuned and those solutions whose energies do not match the constraint are discarded. Usually, the energy of the unconstrained solution is not far away from the actual one (see the analysis of the experimental data given below), so the incremental search for the suitable β is not so time-expensive and, overall, one has an improvement of both the convergence rate and the accuracy.

In the following, we consider the multimode field obtained by seeded PDC. In this case, the photon distribution is expected to have the form

$$\varrho_n=\frac{(n_{\rm th})^n}{(1+n_{\rm th})^{n+M}}\exp\left(-\frac{|\alpha|^2}{1+n_{\rm th}}\right)L_n^{M-1}\left(-\frac{|\alpha|^2}{n_{\rm th}(1+n_{\rm th})}\right), \tag{8}$$

where $\varrho_n\equiv\varrho_n(n_{\rm th},\alpha,M)$ and $L_n^a(z)$ are the generalized Laguerre polynomials. Equation (8) represents the convolution of M thermal states, all with the same average number of thermal photons $n_{\rm th}>0$ except for the stimulated ones, displaced by a collective amount α. This model will be justified by the experimental

setup described in Section 3. From Equations (1) and (8) we can calculate the 'off' probability $p_0 \equiv p_0(n_{\rm th}, \alpha, M, \eta)$, that is

$$p_0 = \sum_{n=0}^{\infty} (1-\eta)^n \varrho_n(n_{\rm th}, \alpha, M) = \frac{1}{(1+\eta n_{\rm th})^M} \exp\left(-\frac{\eta|\alpha|^2}{1+\eta n_{\rm th}}\right), \quad (9)$$

with η being the quantum efficiency of the on/off photodetector. Notice that, from Equation (9), one can obtain the relevant cases for a Poissonian input photon distribution ($n_{\rm th} \to 0$) and for a multithermal one ($\alpha \to 0$). Thanks to Equation (9), one can evaluate the input state energy $N_{\rm ave} = N^{\rm th} + |\alpha|^2$ (with $N_{\rm th} = M n_{\rm th}$), which to be used as a constraint in the algorithm.

Before the end of this section, it is worth pointing out that if each spatial mode consists of M' *temporal* modes, then the input photon distribution and the 'off' probability are still given by Equations (8) and (9), respectively, but with $\mathcal{M} \to M \times M'$ in place of M.

3. Experimental test

In order to test the reliability of the algorithm reported in Equation (7), we applied it to the reconstruction of a stimulated type-I PDC branch, at different stimulation regimes. In our experiment, whose setup is shown in Figure 1, a continuous wave (CW) argon laser ($\lambda_{\rm pump} = 351.1$ nm) pumps a $5 \times 5 \times 5$ mm type-I β-barium borate (BBO) crystal, generating PDC. Together with the pump beam, a CW Nd:Yag laser ($\lambda_{\rm seed} = 1064$ nm) is injected into the crystal in the proper way to generate stimulated

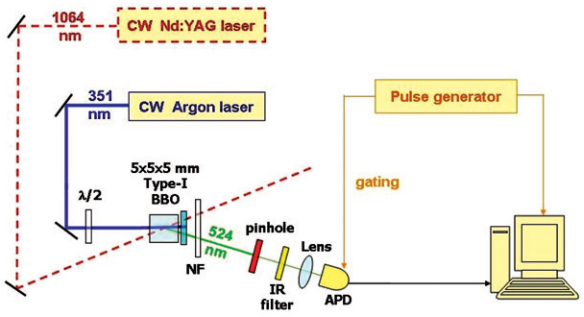

Figure 1. Experimental setup: the stimulated emission at $\lambda_{\rm stimul} = 524$ nm is addressed to the neutral filter (NF) and then collected by the APD. The number and temporal width of the acquisition windows is set by the pulse generator used for the detector's gating. (The color version of this figure is included in the online version of the journal.)

PDC, and we look at the emission in the $k_{\rm stimul}$ direction ($\lambda_{\rm stimul} = 524$ nm).

Different values of quantum efficiency have been obtained by inserting properly calibrated Schott neutral filters (NF), starting from $\eta_{\rm max} = 28.4\%$; after them, on the optical path of the stimulated branch we put an anti-infrared (IR) filter (to cut off the noise due to the Nd:Yag laser dispersion), a variable pinhole (to control the number M of spatial propagation modes collected) and a fiber coupler connected by a multimode fiber with the detector (avalanche photodiode, Perkin Elmer SPCM-AQR-15). We set the pulse generator so that it opens in the avalanche photodiode (APD) 2×10^5 detection windows per second, each one of 20 ns; the pinhole diameter is regulated in order to collect only a few spatial modes (more precisely $M = 7$), of which four are stimulated, as deduced by considering that the stimulated beam generated by our single-mode seed beam concerns four coherence areas of PDC. Moreover, each spatial mode consists of many temporal modes: to evaluate them, we simply divide our acquisition time (20 ns) by the typical coherence time of type-I PDC, obtaining an estimate of the order of magnitude of the total number of modes, i.e. $\mathcal{M} = 7 \times 10^5$. It is worth mentioning that, when the number of modes exceeds a few tens, the dependence on this parameter is rather small and a rough estimate of the order of magnitude suffices.

We have performed three separate data collections, each one corresponding to a different stimulation regime: by indicating with x the percentage of stimulated emission on the whole PDC amount collected, our acquisitions were, respectively, characterized by $x = 51.4\%$, $x = 78.1\%$ and $x = 90.7\%$. The x parameter was estimated by means of the formula $N_{\rm tot} = N_{\rm sp} + xN_{\rm tot}$, with $N_{\rm sp}$ and $N_{\rm tot}$ being the counts given by the ungated detectors with seed off (spontaneous PDC only) and on, respectively. The evaluation of the background photons was performed through an acquisition step without PDC emission (argon pump off, Nd:Yag seed on), followed by a proper subtraction from data.

The obtained results are shown in Figure 2: for the reconstruction we used the MaxLik estimation with a constraint on the energy, as described in the previous section. The plots on the left show the f_0 non-click frequencies given by the stimulated PDC with different stimulation regimes vs. the quantum efficiency η, and the fit obtained by means of the MaxLik estimation and Equation (9). The χ^2 quantity reported has been defined as the sum of the square differences between the 'off' probabilities given by the reconstructed photon statistics and the

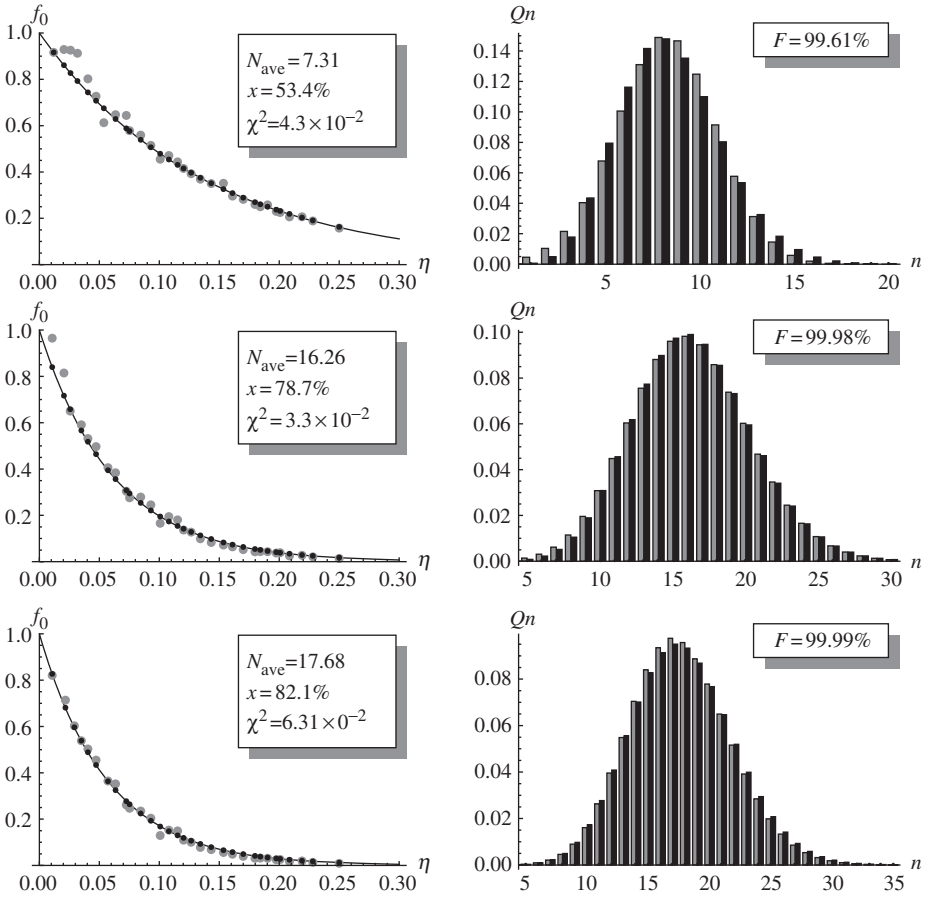

Figure 2. On the left: f_0 non-click frequencies (gray disks) given by the stimulated PDC with different stimulation regimes as functions of the quantum efficiency η. The black disks are the 'off' probabilities obtained by means of the MaxLik reconstructed photon distribution; the solid line corresponds to Equation (9) with $N_{th}=(1-x)N_{ave}$, $|\alpha|^2=xN_{ave}$ and $M=7\times10^5$. In each plot we report also the average number of photons (N_{ave}) obtained by the fit of the experimental f_0, the percentage of stimulated emission x and the χ^2 of the MaxLik fit. On the right: MaxLik reconstructed photon distribution (gray bars) and photon distribution given by Equation (8) with the same values of the parameters given in the respective left plots. In each plot we report also the fidelity F between the two photon distributions. Note the different ranges of n. The corresponding values of the Lagrange multiplier β are (from top to bottom) $\beta=1.95\times10^{-2}$, 1.23×10^{-2}, and 7.40×10^{-3}.

measured f_0. To quantify the similarity between the MaxLik reconstructed photon distribution $\varrho_n^{(ML)}$ and the ϱ_n's obtained from Equation (8), we used the fidelity

$$F=\sum_n\sqrt{\varrho_n^{(ML)}\,\varrho_n}. \tag{10}$$

In Figure 3 we consider the same scenario giving the bottom plots of Figure 2, but now we try to perform the reconstruction without any constraint on the energy ($\beta=0$). We can see that, even if the MaxLik fit of the f_0 frequencies (left-hand side) is good, the fidelity between the MaxLik reconstructed photon distribution and the one given by Equation (8) is quite low (right-hand side): a result that confirms the advantage of using the constrained MaxLik method.

4. Concluding remarks

In this paper we have shown how an important improvement on the convergence of the photon statistics reconstruction code, based on MaxLik estimation applied to on/off detection data, can be achieved by increasing the number of Lagrange multipliers when some *a priori* knowledge of the state is available. In particular, we have addressed the reconstruction of the full photon distribution of multimode fields generated by seeded PDC, demonstrating the advantages of the constrained MaxLik method.

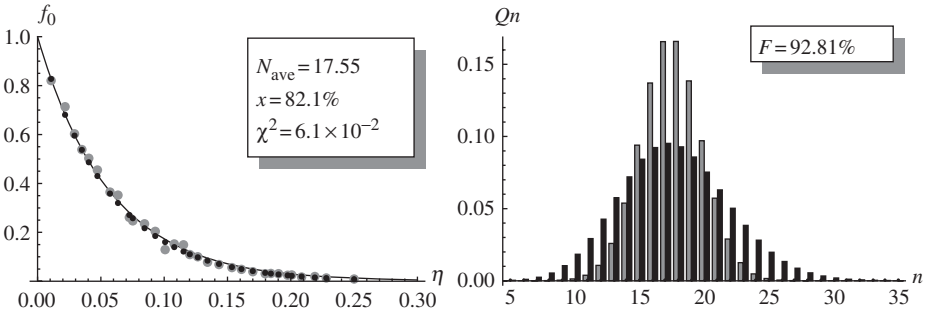

Figure 3. The same plots as in the bottom of Figure 2, obtained without the energy constraint (i.e. $\beta = 0$) on the algorithm (notice that here $N_{ave} = 17.55$, whereas previously it was $N_{ave} = 17.68$ with $\beta = 7.40 \times 10^{-3}$): even if the MaxLik fit of the experimental f_0 set is good, the fidelity between the MaxLik reconstructed photon distribution and the one given by Equation (8) is quite low.

This achievement represents an important step in view of widespread application of this scheme.

Acknowledgements

This work has been partially supported by the CNR-CANIS convention, by Regione Piemonte E14 contract and by 07-02-91581-ASP.

References

[1] Bouwmeester, D.; Ekert, A.K.; Zeilinger, A. *The Physics of Quantum Information: Quantum Cryptography, Quantum Teleportation, Quantum Computation;* Springer: New York, 2000.
[2] Genovese, M. *Physics Reports*. **2005,** *413* (6).
[3] Vogel, W.; Welsch, D.G. *Quantum Optics – An Introduction;* Wiley-VCH: Berlin, 2001.
[4] Schleich, W.P. *Quantum Optics in Phase Space;* Wiley-VCH: Berlin, 2001.
[5] Perina, J.; Hradil, Z.; Jurco, B. *Quantum Optics and Fundamental Physics;* Kluwer: Dordrecht, 1994.
[6] Leonhardt, U. *Measuring the Quantum State of Light;* Cambridge University Press: Cambridge, 1997.
[7] Mandel, L.; Wolf, E. *Optical Coherence and Quantum Optics;* Cambridge University Press: Cambridge, 1995.
[8] Zambra, G.; Bondani, M. *Rev. Sci. Instrum*. **2004,** *75,* 2762–2765.
[9] Kim, J.; Takeuchi, S.; Yamamoto, Y. *Appl. Phys. Lett*. **1999,** *74,* 902–904.
[10] Peacock, A.; Verhoeve, P.; Rando, N.; van Dordrecht, A.; Taylor, B.G.; Erd, C.; Perryman, M.A.C.; Venn, R.; Howlett, J.; Goldie, D.J.; Lumley, J.; Wallis, M. *Nature*. **1996,** *381,* 135–137.
[11] Zappa, F.; Lacaita, A.L.; Cova, S.D.; Lovati, P. *Opt. Eng*. **1996,** *35,* 938–945.
[12] Achilles, D.; Silberhorn, C.; Liwa, C.; Banaszek, K.; Walmsley, I.A. *Opt. Lett*. **2003,** *28,* 2387–2389.
[13] Di Giuseppe, G.; Sergienko, A.V.; Saleh, B.E.A.; Teich, M.C. *Proc. SPIE*. **2005,** *5105,* 39–50.
[14] Munroe, M.; Boggavarapu, D.; Anderson, M.E.; Raymer, M.G. *Phys. Rev. A* **1995,** *52,* 924–927.
[15] Zhang, Y.; Kasai, K.; Watanabe, M. *Opt. Lett*. **2002,** *27,* 1244–1246.
[16] Raymer, M.; Beck, M. *In Quantum States Estimation; Lecture Notes in Physics 649;* Springer: Berlin-Heidelberg, 2004; pp 235–295.
[17] Mogilevtsev, D. *Opt. Comm*. **1998,** *156,* 307–310.
[18] Mogilevtsev, D. *Acta Phys. Slov*. **1999,** *49,* 743–748.
[19] Rossi, A.R.; Olivares, S.; Paris, M.G.A. *Phys. Rev. A* **2004,** *70,* 055801-1–4.
[20] Rossi, A.R.; Paris, M.G.A. *E. Phys. Jour. D* **2005,** *32,* 223–226.
[21] Zambra, G.; Andreoni, A.; Bondani, M.; Gramegna, M.; Genovese, M.; Brida, G.; Rossi, A.; Paris, M.G.A. *Phys. Rev. Lett*. **2005,** *95,* 063602-1–4.
[22] Gramegna, M.; Genovese, M.; Brida, G.; Bondani, M.; Zambra, G.; Andreoni, A.; Rossi, A.R.; Paris, M.G.A. *Laser Physics*. **2006,** *16,* 385–392.
[23] Brida, G.; Genovese, M.; Gramegna, M.; Paris, M.G.A.; Predazzi, E.; Cagliero, E. *Open Syst. & Inform. Dynam*. **2006,** *13,* 333–341.
[24] Brida, G.; Genovese, M.; Piacentini, F.; Paris, M.G.A. *Opt. Lett*. **2006,** *31,* 3508–3510.
[25] Brida, G.; Genovese, M.; Paris, M.G.A.; Piacentini, F.; Predazzi, E.; Vallauri, E. *Opt. Spectrosc*. **2007,** *103,* 95–102.
[26] Banaszek, K. *Phys. Rev. A* **1998,** *57,* 5013–5015.
[27] Hradil, Z.; Mogilevtsev, D.; Řeháček, J. *Phys. Rev. Lett*. **2006,** *96,* 230401-1–4.
[28] Olivares, S.; Casagrande, F.; Lulli, A.; Paris, M.G.A. *EPL*. **2007,** *80,* 64002.